Global Advanced Research Journal of Agricultural Science (ISSN: 2315-5094) Vol. 8(3) pp. 090-100, March, 2019 Issue.
Available online http://garj.org/garjas/home

Full Length Research Paper

Biosynthesized of zinc oxide nanoparticles using Aspergillus *terreus* and their application as antitumor and antimicrobial activity

Dina El-Kahky[1], Magdy Attia[2], Saadia M Easa[1], Nemat M. Awad[2] and Eman A. Helmy[3]

[1]Microbiology Department, Faculty of Science, Ain Shams University, cairo, Egypt
[2]Agricultural Microbiology Department, National Research Centre, 33 El-Bohouth Street, (former El- Tahrir Street) Dokki, Giza, Egypt. Postal Code: 12622
[3]Microbiology Department, The Regional Center for mycology and Biotechnology, Al-Azhar University, cairo, Egypt

Accepted 09 March, 2019

This study is refers to identify an easy and eco-friendly way for biosynthesis of nanoparticles of zinc oxide and that is done by utilizing extracts from *Aspergillus terreus* as well as trying to identify their effectiveness in antibacterial and antimicrobial activities. A test is performed for zinc oxide nanoparticles on some types of gram positive and gram negative bacteria were tested by disc diffusion method against on Luria-Bertani agar media and the antitumor activity of HCT-116 (colon carcinoma cell) cancer cells. The zinc oxide nanoparticles which is synthesized by *Asperagillus terruus* were characterized by "UV spectro", Transmission Electron Microscopy "TEM" showed spherical shape and smooth surfaces with an size of about 110 nm, X-ray Diffraction "XRD", FTIR spectra of synthesized zinc oxide nanoparticles exhibited prominent peaksat 34440.39 cm^{-1} (NH stretching), 1639.02 cm^{-1} (N-H bend primary\ amines), 3230.18 cm^{-1} (amide), 595.896 cm^{-1} (O-H hydroxyl group) and 638.323 cm^{-1} (=C-H). The characterization shape of their synthesis. The best zone of inhibition was determined in the synthesized zinc oxide nanoparticles (9.7 mm) against *Staphylococcus aureus* (28.3 mm) *Escherichia coli*, MRSA (13.0 mm) and *Pseudomonas aeruginosa* (17.7 mm).The result showed that synthesized Zinc Oxide nanoparticles are more antibacterial effect than the standard antibiotic disk, Ampicillin Synthesized Zinc Oxide nanoparticles were found law antitumor activity of HCT-116 cancer cells with a IC_{50} value of 0.7 µl. It provide an approach investigator can meet the requirement of large and wide scale of industrial production with the advantage of low cost, eco-friendly and reproducible.

Keywords: antibacterial, antitumor, *Aspergillus terreus,* bacteria, biosynthesis, human pathogenic nanoparticles.

INTRODUCTION

For creating a new way and a new vision for the researchers it is blended between nanotechnology and biological science to create the new path for profiteering in various biological fields. At present, the synthesis of

nanoparticles is becoming increasingly important in nanotechnology research because of its enormous applications in medicine, biomedicine, medicine, drug delivery, and catalytic activity (Basn et *et al.,* 2019). In ancient times, there was an increase in demand for metallic nanoparticles that can be collected and synthesized through several physical and chemical processes in various traditional shapes and sizes. The disadvantages of the physical method include treatment at high temperature and pressure, requiring a large area for machine preparation, and high cost (Chandrasekaran *et al.,* 2016). On the other side, it is hazardous and dangerous to workers and also the environment utilizing dangerous and harmfully materials like reducing agents, organic solvents, and stabilizers in the chemical approach during installation. It is observed that the toxicity of the substances within nanoparticles if they are done either in a physical or chemical way that stimulates risks in their applications. Furthermore, use zinc oxide nanoparticles in a lot of applications increases the toxic risk for its appearing to the environment (Sharmila *et al.,* 2017).The green approach, which allows wide scale for production of nanoparticles, is considered the other way to synthesize nanoparticles in an eco-friendly, biocompatible, safe, and cost-effective through the use of bacteria, fungi, algae, and plants. Mostly fungi were chosen instead of bacteria because of their tolerance, better metal bioaccumulation ability, and high binding capacity. There are wide applications of fungi as they produce huge enzymes, ease in the scale-up process, economic viability, and ease in handling the biomass (Happy *et al.,* 2017)

The goal is the establishment of new technology by using biosynthesis zinc oxide nanoparticles for antitumor and antibacterial activity which enhance the efficiency of existing requirement and reduce discharge and its contribution to the global community. Therefore, the antitumor effect of zinc oxide nanoparticles has been investigated on human breast adenocarcinoma cell line HCT-116 (colon carcinoma cell) cancer.

MATERIALS AND METHODS

Biosynthesis of zincoxide nanoparticles by fungi isolates

Four isolates namely AG 16, AG19, TFO, and AG20 were selected for their growth and production of pigment in Czapek-Dox agar medium supplemented with different concentrations of zinc oxide (0.5, 1.0, 1.5, 5.0 and 10 mM) in order to further determine the most efficient tolerate strains to high concentrations of zinc oxide. To prepare biomass for biosynthesis studies, the fungi were grown aerobically in a modified Czapeck-Dox liquid media in 250 ml Erlenmeyer flasks containing 100 ml liquid media in each flask. The flasks were inoculated and incubated on an orbital shaker at 28±2 °C and agitated at 150 rpm. After 5 days, by using sieving through a plastic sieve, the biomass was harvested allowed by extensive washing with Milli-Q deionized water to disappear any other medium component from the biomass. Twenty grams of *Aspergillus terreus* fresh biomass was collected in contact with 100 ml of Milli-Q deionized water for 72 hrs at 28±2 °C in an Erlenmeyer flask and agitated in the same condition as described before. The cell filtrate was obtained by passing through the filter paper Whatman No. 1 after incubation for the cell.

Preparation of stock solution of zinc oxide

The stock solution of the zinc oxide was prepared by dissolving 0.00813 g/L of zinc oxide in 20 ml of sterilized distilled water to get the 5 mM concentration and then stored for use in experimentations.

Extracellular production of zinc oxide nanoparticles

Production of nanoparticles was done according to the method of (Ghareib *et al.,* 2015). Zinc oxide 5 mM was mixed with 50 ml of cell filtrate of *Aspergillus terreus* in a 250 ml Erlenmeyer flask and moved it for 5 minutes. Control treatment (without the ion) was also run along with the experimental flask and the absorbance was measured at a resolution of 1 nm using a UV–Visible spectrophotometer (UV-2401 PC) at ca. 377 (zinc oxide).

Method for Identification of the fungal isolate

Morphological and microscopic observations were carried out for identification of the selected fungal isolate followed by 18S rRNA gene sequencing according to (Amutha and Godavari 2014). The resulting sequence was analyzed using the BLAST algorithm of The European Molecular Biology Laboratory-The European Bioinformatics Institute (EMBL-EBI) database to obtain closely related phylogenetic sequences. The phylogenetic tree was constructed using the Neighbour-Joining method in Clustal omega software graph (Hinrikson *et al.,* 2005).

Optimization of substrate concentration for biosynthesis of ZnO nanoparticles

For the synthesis of zinc oxide nanoparticles, different concentrations (0.5, 1, 1.5, 5, 10 mM) of zinc oxide was mixed with 50 ml of cell filtrate in a 250 ml Erlenmeyer flask and incubated for 72 hrs at 28±2 °C in dark. Control without ions was also run along with the experimental flask. A sample of 1ml was withdrawn after 72 hrs and the

*Corresponding author's E-mail: d_elkahkey@yahoo.com

absorbance was measured at a resolution of 1 nm using a UV–Visible spectrophotometer (UV-2401 PC) at ca. 377 (zincoxide).

Characterization of zinc oxide nanoparticles UV-Vis Spectrophotometer Studies

The reduction of zinc oxide nanoparticles was monitored by measuring the UV-Vis spectrum of the reaction medium at different range (200 nm to 800 nm) by drawing 1cm of the samples and their absorbance was recorded at a resolution of 0.5 m using UV-Vis spectrophotometer (UV-2401 PC).

Method of Fourier Transform Infrared Spectroscopy Analysis (FTIR)

Potassium Bromide (KBr) was mixed with the dried zinc oxide nanoparticles vacuum at a ratio of 1:100. The spectra were determined with a system named SHIMADZU 8400S Fourier Transform Infrared Spectrophotometer which using a reflectance accessory diffuse. The scanning data were determined by the average of scans in about 4000 to 400 cm^{-1}.

Use Transmission Electron Microscope (TEM)

The cell filtrates of *Aspergillus terreus* isolate was utilized to form a film of zinc oxide nanoparticles on carbon-coated copper grids and analyzed under (TECNAI 120) Transmission Electron Microscope at a range of volt as 120 kV (Williams, 1996).

Use X-Ray Diffraction Analysis (XRD)

For measuring X-Ray Diffraction the liquid solution of zinc oxide nanoparticles mixture after bio reduction was collected and dried at 45 ºC in a vacuum drying oven. After that, the dried mixture of zinc oxide nanoparticles was collected for the observation of the structure of zincoxide nanoparticles. The spectra were recorded from the X-Ray system according to WIN-FIT program.

Method of purification of the protein

For solutions which containing proteins, solid ammonium sulphate was added slowly, this is for controlling liquid solutions containing extracellular proteins at a final concentration of 80 % (w/v), then after that, the step of purification of proteins from aqueous cell-free filtrate is done. The precipitate fraction was subsequently dialyzed by utilizing a 12-kDa cut-off membrane. The mixture was stirred gently for overnight at 4 ºC. Then the precipitate was collected by centrifuge the precipitated mixture at 1200 rpm for 10 minutes at 4 ºC.

Use of Electrophoresis of the native protein (PAGE)

A mixture of protein extract supernatant is prepared with an equal volume of a solution this liquid solution containing 0.1 ml bromophenol blue in 0.15 M Tris-HCl and 20 % glycerol (v/v) and this mixture of solution pH is blended at 6.8. 20 microliters of the residual suspension (40 to 60 µg of protein) were adjusted to electrophoresis in 25 mM Tris buffer containing 190 mM glycine and the mixture of solution pH is blended at pH 8.3. The dye band conducted at the bottom of the separating gel where Electrophoresis was at 10 °C for 4 hours in a 7.5 % polyacrylamide gel with a 3.5 % stacking gel, at 15 and 30 minute. In a straight style, until the dye band is appeared. Electrophoresis was performed in a vertical slab mould (16x18x0.15 cm). Gels were stained with silver nitrate for the detection of protein bands (Sammons *et al.,* 1981).

Method of Gel analysis

Protein patterns obtained by Electrophoresis of native protein was clustered by gel documentation system (Uvitec, Cambridge, UK) by the µn weighted pair group method of arithmetic means (UPGMA) according to Sneath and Sokal (1973). The same way coefficient matrix among protein banding patterns was calculated based on the number of shared bands (Nei and Li, 1979).

For Protein Analysis Using MALDI-TOF/TOF profiling measurements, each defatted, diluted sample was mixed 1:1with distilled water (Bruker Daltonics, Bremen, Germany).

Application studies of the produced nanoparticles Evaluation of antibacterial activity Microorganisms used in this study (Tested organisms)

Antibacterial activity was carried out using four different strains, namely included, the bacteria Gram-negative bacteria [*Escherichia coli* O157H7 &*Pseudomonas aeruginosa* ATCC10145] and Gram-positive bacteria [*Staphylococcus aureus* NRC 23516 and Methicillin-resistant *Staphylococcus aureus* (MRSA) NRC 629012]. The cultures were packaged from Agriculture Microbiology Department, National Research Centre Dokki, Cairo, Egypt. All bacterial strains were stored as frozen stocks at -80°C (Protect Bacterial Preservation System, Technical Service Consultants), and maintained on Luria Agar (LA) medium at 37 °C.

Bacterial culture

Bacterial culture was carried out in Luria Broth "LB" or solid agar medium, Luria Agar media "LA", contained 1.5 % "w/v" of standard microbiological agar. LB and LA were sterilized by using autoclave at 121 °C for 20 minutes. All

liquid cultures or liquid media were incubated in an aerobic way on a rotary shaker at 37 °C, at 200 rpm.

Bacteriostatic activity

The bacteriostatic activities of zinc oxide nanoparticles were investigated by the disc diffusion method (Jeevan *et al.* 2012). LB agar plates were prepared, sterilized and solidified, after that, bacterial cultures were swabbed. ZnO nanoparticles solution with different concentration (6.25µl, 12.5µl, 25µl, 50µl,and 100µl) located in the agar plate, then collected and reserved for incubation at 37 °C for 24 hours. Zone of inhibition was determined, measured and compared with control (cell-free water extract).

Determination of the antitumor activity of zinc oxide Nanoparticles

Antitumor effect of zinc oxide nanoparticles synthesized by fungal extract was identified in vitro against HCT-116 (colon carcinoma) cell line which was kindly received from VACSERA Tissue Culture Unit. Appropriates dilutions of zinc oxide nanoparticles were tested as an antitumor effect in vitro by trypan blue exclusion method reported by Caixia *et al.* (2015).

Method of Statistical analysis

All Conduct analysis of statistics was performed using SPSS “Statistical Package for the Social Sciences” software package (SPSS In. the U.S.A.) and Excel (Microsoft, U.S.A.). The result data were subjected to analysis of variance, and significant differences between means were observed by Duncan’s multiple range tests ($p < 0.05$).

RESULT

Efficient Metal tolerance assay

The differences concentration of zinc oxide (10mM) was affected the growth of four fungal isolates inoculated in the Czapek-Dox solid medium supplemented with zinc oxide after five days of growth. The isolate AG 16 had shown growth till 10 mM. The fungal isolatesTFOand AG19 were unable to grow even at 5mM. Whereas, AG20fungal isolate was grow increasingly at lower concentrations (0.5 and 1.0 mM) covering entire Petri dish, but at 5.0mM it was unable to grow. The isolate AG16 was exhibiting higher metal tolerance.

Production pigments

Four isolates were screening for their ability to synthesis ZnO nanoparticles from Zinc oxide. The fungal biomass was separated by filtration after the incubation period of 72 hrs. The pale white colour of the aqueous cells solution can clearly be observed in the bottle containing the aqueous cells solution after immersion in 10mM zinc oxide solution for 24 hrs. The appearance of a pale white colour in solution containing the biomass was suggested as indicator of the formation of zinc oxide nanoparticles in the reaction mixture (Figure 1).

The Ultraviolet and Visible of zinc oxide nanoparticles production by the four isolates was observed in Figure 2. The strong surface plasmon resonance centered at about ca.377 nm was determined for zinc oxide nanoparticles extracellular from four isolates after 72 hours of incubation and intensity of the peak was increasing as the top of the reaction continues which determine an increase in the of zinc oxide nanoparticles numbers. Intensity has not appeared any changing at around ca.377 nm which indicate complete reduction of zinc oxide ions. It was observed that there was absorption ranges at 270 nm demonstrate the presence of protein residues as species tryptophan and tyrosine in them. While, in case of negative control (zinc oxide solution alone), the change in colour not happened was determined even after 72 hours and also even after 10 days. The isolate AG 16 was selected for further study.

Identification of selected isolate

Fungal isolate AG 16 ability to synthesis zinc oxide nanoparticles was analyzed taxonomically. The colony on PDA is brownish in colour and gets darker. Conidial heads that is compact, biseriate, and densely columnar. This fungus is readily distinguished by its cinnamon-brown colony coloration and its production of aleurioconidia. Selected fungus isolates were further identified on the basis of sequence analysis of 18S rRNA and phylogenetic tree. The isolate *Aspergillus terreus* has typical characteristics to *Aspergillus terreus* strain RA106. The fungal genomic DNA fragment in the region 5S–28S is registered in GenBank with acc. No. KU14241.1 (Figure 3).

Effect of substrate (zinc oxide) concentrations on the synthetic ZnO nanoparticles

The effect of different concentrations of zinc oxide (0.5, 1, 1.5, 5.0, 10.0 mM) was studied for synthesis the ZnO NPs. The cell filtrate was treated with different concentration of zinc oxide and incubated. The maximum concentration used was 10 mM and the best production concentration was determined at 5 mM concentration as shown in Figure 4 and 5.The extra cellular biosynthesis of zinc oxide nanoparticles is done within 72 hours of incubation with zinc oxide ions.

Figure 1: Colour change of culture supernatant from yellow to white colour after 24 hours of reaction isolates with zinc oxide

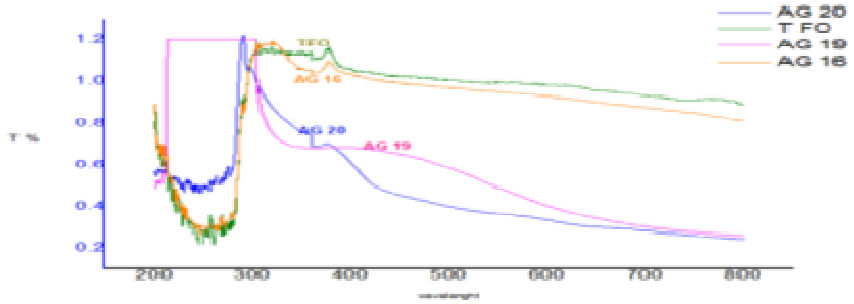

Figure 2. Ultraviolet and Visible spectra recorded after 72 hours of the reaction of a 10 mM of Zinc oxide solution with the culture supernatant of isolates AG 16, AG19, TFO, and AG20.

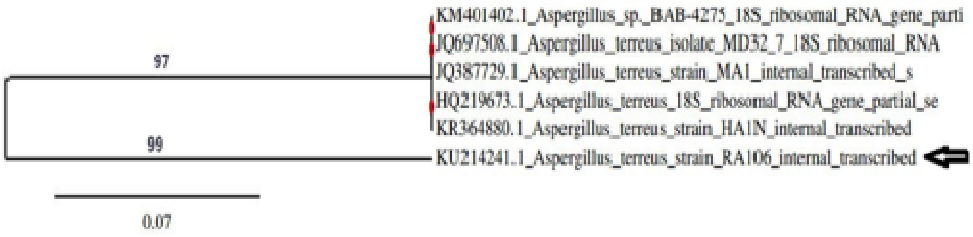

Figure 3: 18S ribosomal RNA gene Phylogenetic tree of the identified MP strain *Aspergillus terreus.*

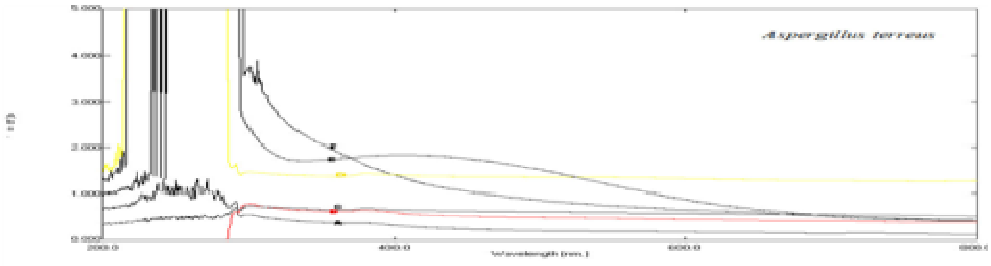

Figure 4: Ultraviolet and Visible spectra recorded after 72 hours of reaction of an solution for “0.5, 1, 1.5, 5.0, 10.0 mM” zinc oxide with the extra cellular components of *Aspergillus terreus* A = control, B = 0.5 mM, C = 1 mM, D = 1.5 mM, E = 5mM, F = 10 mM.

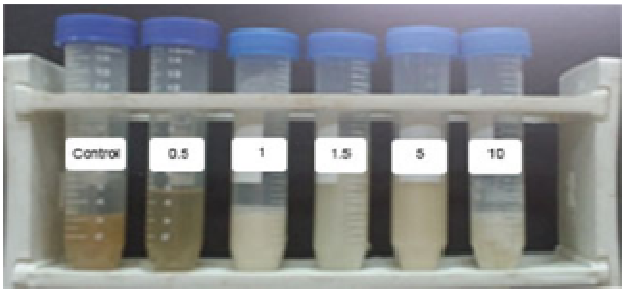

Figure 5: Photograph of different substrate concentrations after 72 hours of the reaction of a solution of (0.5, 1, 1.5, 5.0 and 10mM) zinc oxide with the extra cellular components of *Aspergillus terreus*

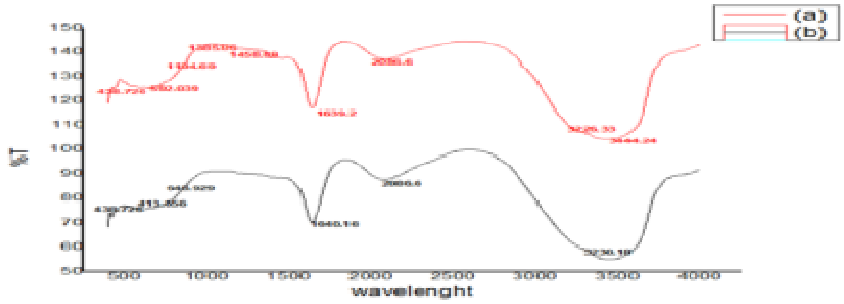

Figure 6: FTIR recorded from spectra of Zinc Oxide nanoparticles synthesized by culture supernatant of *Aspergillus terreus* (a) and fungal extracted (b)

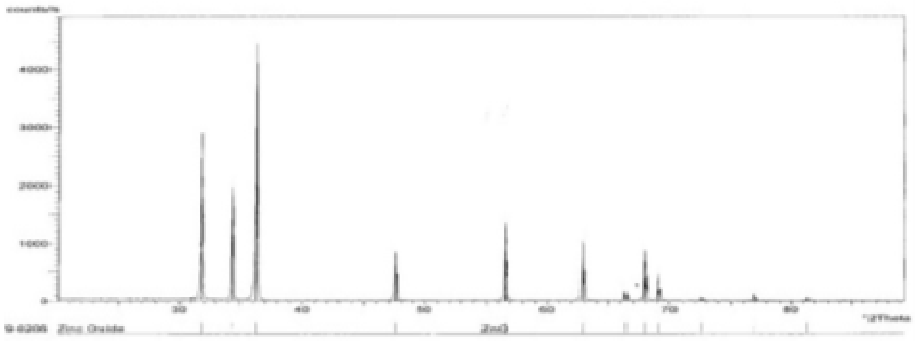

Figure 7 X-ray diffraction pattern of the dried ZnO nanoparticles production by extracellular components of *Aspergillus terreus*.

Fourier-transform infrared spectroscopy spectrum of *Aspergillus terreus* extract and zinc oxide nanoparticles

Figure 6 represents the Fourier-transform infrared spectroscopy spectra of Zinc oxide nanoparticles synthesized by *Aspergillus terreus* curve (a) and *Aspergillus terreus* extract curve (b). The two curves show that there was a variation in the intensity of bands at different regions. Curve (a) indicates the characteristic band of free OH group at 3444.24 cm^{-1} and 3226.33 N-H stretching for primary, secondary amines. 2086.6 NH stretching Amide B, 1639.2 N–H bend primary amines, 1458.89 symmetric stretching vibrations of -COO, 1385.06 residual NO_3-.1194.69 secondary aliphatic amines a major peak was identified at 592.03 cm^{-1} corresponds to the =C–H bending, in addition, the band at 438.72 cm^{-1} reveal the oxygen stretched bond. From Curve (b) a major peak was identified at 3230.18 and 2086.6 cm^{-1} corresponds to the N-H stretching for primary, secondary amines. A major peak was identified at 1640.16 cm^{-1} corresponds to the stretch vibration of C=C. This shifting of the peak from 648.929 to 438.726 cm^{-1} indicates =C-H bending and oxygen stretched bond.

X-Ray Diffraction Analysis (XRD)

The purity of the phase and composition of the products obtained by the biosynthesis zinc oxide nanoparticles using an extract of *Aspergillus terreus* examined by X-Ray Diffraction. Figure 7 observes a typical X-Ray Diffraction pattern of zinc oxide nanoparticles in about 30- 80° at a

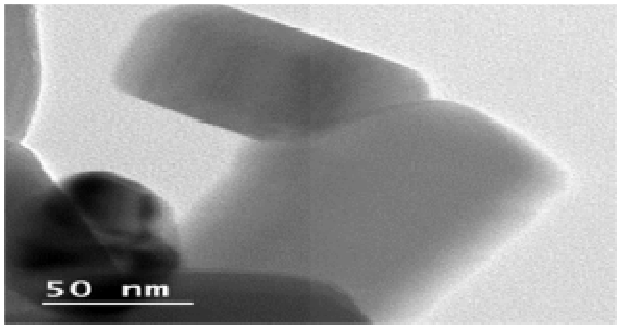

Figure 8. Analysis of TEM micrograph of *Aspergillus terreus*

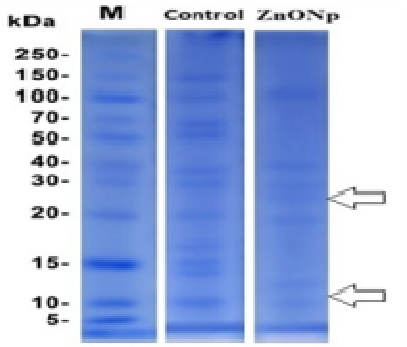

Figure 9 The profile of extra cellular proteins secreted by *Aspergillus terreus*

scanning step of 0.01. A number of Bragg reflections with 2θ values of 31.717°, 34.367°, 36.201°, 47.483°, 56.690°, 67.894°,and 68.105° are observed corresponding to (100), (002), (002), (001),(001), (001) and (001) planes, shows a typical XRD pattern of zinc oxide nanoparticles in the range of 0-80° with Philips Analytical X-Ray Diffraction.

Transmission electron microscopic (TEM)

From the Transmission electron microscopy is observed in Figure 8 the particles obtained show a regular cubic shape with smooth surfaces and the size was distributed in a range of about 70-130 nm.

Protein purification

The protein fraction clearly showed the presence of intense bands of 69, 51, 20, 17, 15, 13 and kDa (bands highlighted by arrows in Figure 9, lane control. Zinc oxide nanoparticles also bands at 28, 27, 13 and 10 KDa. These proteins can be demonstrated responsible for the synthesis as well as the stability of zinc oxidenanoparticles.

Protein analysis using MALDI-TOF

Figure 10 shows the MALDI-TOF the peak were determined to be around *m/z* 2068, 2107, 2582, 3601, 4684 and 6319 with appeared the absence of *m/z* shift from control (cell filtrate) 1718, 3601 and 1882 suggested zinc oxide nanoparticles preparation.

Application of ZnONPs as an antibacterial andanantitumor Bacteriostatic activityusing disc-diffusion method (mm)

To test the antibacterial activity for the zinc oxide nanoparticles was carried out using four different human pathogenic bacterial strains. The microorganisms were Gram-negative "*Escherichia coli*; *Pseudomonas aeruginosa*" and Gram-positive *"Staphylococcus aureus*; MRSAMethicillin-resistant *Staphylococcus aureus*". The antibacterial activity was assayed on LBA plates using different concentrations of zinc oxide nanoparticles (6.25µl, 12.5µl, 25µl, 50µl, 100µl). The disc-diffusion method using

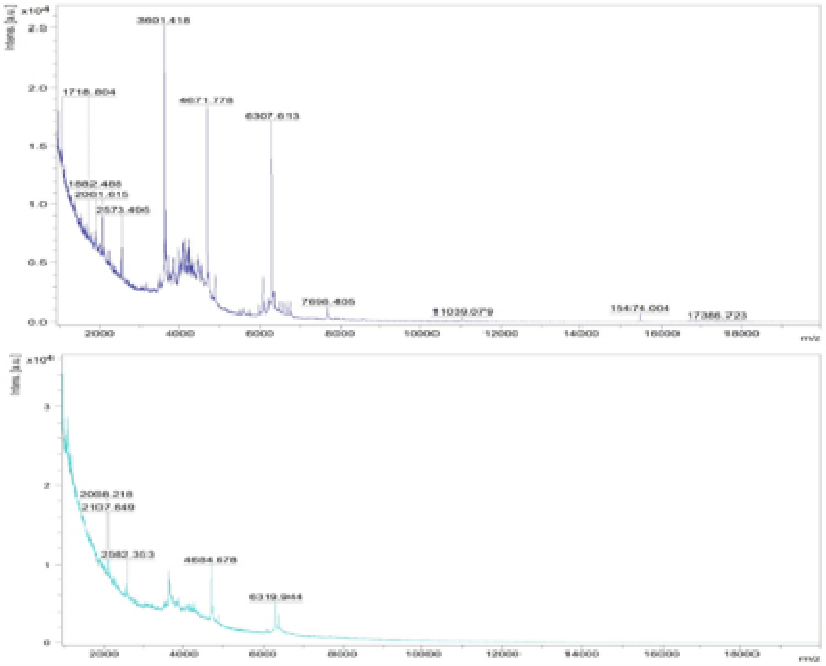

Figure 10: Analysis of extra cellular proteins *Aspergillus terreus* before and after treated biosynthesis of Zinc oxide Nanoparticles (ZnONPs) using MALDI-TOF

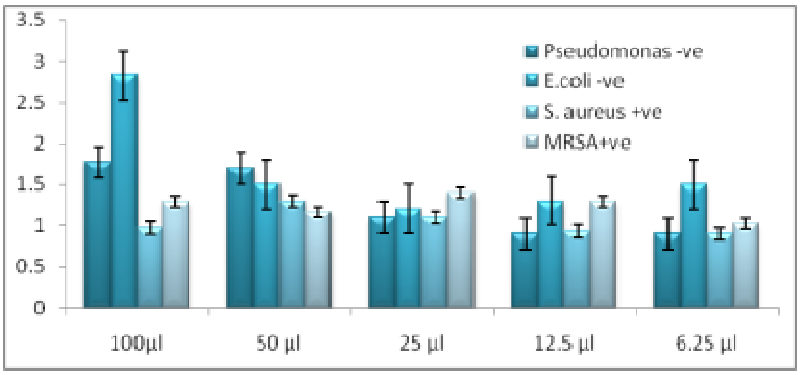

Figure 11: Antimicrobial effect of nanoparticles, nano composite produced against human pathogenic microbes, data showing increasing inhibition zone with increasing amounts of nanoparticles; clockwise from top: 6.25µl, 12.5µl, 25µl, 50µl, 100µl with volume madeup to 100 µl with distilled water wherever needed. zinc oxide nanoparticles (ZnONPs)

and the inhibition zones of the different pathogenic microbes were measured. The inhibition zone caused by zinc oxide nanoparticles gradually increased with *Escherichia coli*; and *Pseudomonas aeruginosa* (Gram-negative) compared with *Staphylococcus aureus* and *MRSA* (Gram-positive). However, no inhibition zones were visible in the cell-freefiltrate water extract alone (Table 1).

Figure 11 and Table 2 show that all the four tested microbes that were tested were inhibited at low concentrations of nanoparticles. The inhibition zones were gradually increased with increasing concentration of nanoparticles against Gram-negative "*Escherichia coli*; *Pseudomonas aeruginosa*" and Gram-positive *"Staphylococcus aureus*; MRSAMethicillin-resistant *Staphylococcus aureus"*.

Tissue Culture

Zinc oxide Nanoparticles were examined for their cytotoxicity effect in vitro by determination of the number of surviving cells by staining with crystal violet of HCT-116 (colon carcinoma cell) cancer cells observes cell viability after cultivated with Zinc oxide Nanoparticles for 24 hours, together with a control (nanoparticles is disappeared) as a comparison. Viability, measured, showed a dose-

Table 1: The bacteriostatic activities of zinc oxide nanoparticles Although there are differences in the value of averages, it is statistically insignificant

Strain	Control	Zinc Oxide nanoparticles	Antibiotic
	Inhibition zones (mm)		
P. aeruginosa	9.1 ±0.25942	17.7±0.80829	27±0.80829
E.coli	10.67±0.18037	28.3±0.42147	16.1±0.42147
S. aureus	7.7±0.11547	9.7±0.25166	20.3±0.25166
MRSA	10.3±0.41633	13±0.52048	15.7±0.52048

Table 2: The effect of different concentration of Zinc oxide nanoparticles on human pathogenic bacteria

strain / ZnONP	*Pseudomonas -ve*	*E.coli -ve*	*Staph aureus +ve*	*MRSA +ve*
100	17.7±0.80829	28.3±0.42147	9.7±0.52048	13±0.30050
50	17±0.20817	15±0.51733	13±0.46188	11.7±0.26667
25	11±0.34641	12±0.15588	11±0.05774	14±0.03333
12.5	9.0±0.00	13±0.44557	9.3±0.30551	13±0.30551
6.25	9.0±0.00	15±0.50954	9.0±0.00000	10.2±0.0000

Filtrate extracts of *Aspergillus terreus*; Zinc oxide nanoparticles (ZnONPs); SD, although there are differences in the value of averages, it is statistically insignificant

Table 3: Viability and inhibition of HCT-116 cells after 24-hour incubation Treatment with *Aspergillus terreus* as control cell and extra cellular biosynthesized Zinc oxide nanoparticles.

Conc. (µl)	Viability%	
	Aspergillus terreus	**Zinc Oxide nanoparticles**
100	21.77±0.16623	4.47±0.3606
50	76.89±0.91602	10.18±0.7937
25	87.92±0.95567	17.92±0.7211
12.5	96.03±0.33719	26.41±0.3464
6.25	99.87±0.15395	31.38±0.7550
3.125	100±0.0000	36.56±0.17692
1.56	100±0.0000	42.68±0.1732
0.78	100±0.0000	48.34±0.1732
0.39	100±0.0000	56.73±0.2309
0.2	100±0.0000	65.08±0.38158
0	100±0.0000	100±0.0000

Literate extract of *Aspergillus terreus*; Zinc oxide nanoparticles (ZnONP); SD, Although there are differences in the value of averages, it is statistically insignificant

dependent decrease at a very low concentration with IC_{50}= 0.7µl (Table 3).

DISCUSSION

The isolates namely AG16, AG19, TFO, and AG20 collected from 3 different sites have reacted with zinc oxide

the isolate AG16 AG19, TFO and AG20 were selected at about ca.377, 389, 387, and 380 respectively. Where the best strong surface plasmon resonance cantered at ca.377 nm was determined for the isolate AG16 zinc oxide nanoparticles produced. The zinc oxide nanoparticles which produced were analyzed using Ultraviolet and Visible spectrum. The zinc oxide nanoparticles absorption peaks determined should be between 340-385 nm and the maximum production when using different concentrations was observed at 5 mM concentration. Ultraviolet and visible spectroscopic studies determined that the surface plasmon resonance, sure to be the reduction of metal ions and preparing of nanoparticles with a peak at 350 nm (Rajan *et al.* 2016). Method of Identification of selected isolate. In spite of, results by Chang and Ehrlich (2010) determined that the characteristics morphology which used to distinguish between *Aspergillus flavus* and *Aspergillus oryzae* can be subtle and can lead to misidentification. Generally, It is possible to use microscopic and macroscopic characteristics of colony colour and conidial sizes to distinguish between *Aspergillus flavus* from *Aspergillus oryzae.* In spite of *Aspergillus flavus* and *oryzae* from corn grains isolates were divided into two subclades, separated "*Aspergillus flavus* NRRL1957 and *Aspergillus oryzae* NRRL447" were became in a group together. Chang and Ehrlich have observed that *Aspergillus flavus* and *Aspergillus oryzae* were genetically close related, similar and have a phylogenetic association related to each other (Chang and Ehrlich 2010). Kurtzman *et al.* observed that a lot of β-tubulin, calmodulin and to poisomerase II including genes have a low variability to separate *Aspergillus flavus* and *Aspergillus oryzae*, and determined that regulatory gene locus, of infra-red or many genes structured be used to make the two closely related species are separated. Kurtzman *et al.* (1986) also determined that 100% DNA hybridization between *Aspergillus flavus* and *Aspergillus oryzae*, were genetically similar.

Characterization of zinc oxide nanoparticles

The presence of Zinc oxide interaction was determined by the peaks at 1070 cm^{-1} and 860 cm^{-1} which are about peak 979.9 cm^{-1} (Sangappa M. 2013). As result in Figure 6 presence of Zinc Oxide interaction was determined by the peaks at 417.513 cm^{-1} and 413.656 cm^{-1} which are near to peak 438.726 cm^{-1} which represents the FTIR spectra of Zinc oxide nanoparticles synthesized by *Aspergillus terreus* curve. Transmission Electron Microscopy “TEM” visualization which allows determining the shape of nanoparticles and also the size of the zinc oxide observed in Figure 8 in the range of 5-180 nm nanoparticles like formed by (Vijayakumar *et al.,* 2018). Powder of zinc oxide nanoparticleswas used by ray diffract to measure for sure that the appearance of Zinc Oxide and analyze the structure. The graph observed main peaks corresponding to 2θ values of 31.717° and 36.203° in the multiplot determined in Figure 7. The peaks of the graph are in close agreement with the literature (Kumar and Savalgi 2017)

Protein estimation and analysis

In the present study, a single protein band prominent, with molecular weight of 27, 28, 13, 10 kDa Figure 9 was determined and detected to be present in the culture filtrate, secreted out of the fungal biomass and the enzyme protein of Zinc Oxide might have involved in the reduction of the Zinc Oxide ions Nanoparticles related studies also appear in (Navin *et al,* 2010). Spectra were analyzed by the BioTyper program (version 3.1; Bruker Daltonics, Inc.) utilizing both the Bruker database and a previously created NIH database. A logarithmic score cut-off of more or equal 2.00 for applied acceptable identification Identification results was reported at level following laboratory protocols, as in Figure 9, 10 Zinc Oxide nanoparticles protein peptides differences were determined much like a fingerprint.

The toxicity study of different biosynthesized nanoparticleson human diseases bacteria

The antibacterial effect of zinc oxide nanoparticles against several isolates has been reported well such as in *Staphylococcus* sp. MRSA methicillin-resistant *Staphylococcus aureus* sp. (Jesline *et al.* 2015) and *Pseudomonas* spp. (Jiang *et al.*2014), *Escherichia coli* (Zhang *et al.*2014). Similar results of cytotoxicity have been determined by Prasanth *et al.* (2015), including the targeted delivery of Zinc Oxide nanoparticles which become themselves the therapeutic agent or the Zinc Oxide nanoparticles are reacting as carriers for some other agent; in any case of the two cases, biosynthesized Zinc Oxide nanoparticles are becoming important in nanomedicine and still having more new researches. Premanathan *et al.* (2011) their studies show that the primary mechanism of Zinc Oxide nanoparticles 'cytotoxicity may continue to occur inducing the generation of reactive oxygen species as an antioxidant, that is responsible for the induction of apoptosis. Furthermore it, the more research show that the Zinc Oxide nanoparticles were more internalized readily through an endocytosis mechanism upon internalization of Zinc Oxide nanoparticles enhancing the therapeutic effect through exhibiting antiproliferative activities on MCF-7 cell lines at an IC_{50} concentration of about 3.5 µg/mL. These researchgive Suggestions that the size of nanocarriers become with a diameter less than 200 nm this suggestion could be a target tumours effectively in vivo through their enhanced permeability and retention “EPR” effect.

CONCLUSION

Biosynthesis and investigating of zinc oxide nanoparticles and the antibacterial and antitumor properties of these nanoscale composites was one of our goals based on our results. Zinc oxide has a good effect on gram positive and negative bacteria, also HCT-116 (colon carcinoma cell) cancer cells

CONFLICT OF INTEREST

The present study was performed in absence of any conflict of interest.

ACKNOWLEGEMENT

The author would thank all participants.

AUTHOR CONTRIBUTIONS

All authors contributed equally in all parts of this study.

REFERENCE

Amutha K and Godavari A, (2014). Identification of *Aspergillus terreus* using 18S rRNA gene sequence, Asian Journal of Biochemical and Pharmaceutical Research 4: 2231-2560.

Basnet LM, Shrestha S, Sapkota S, (2019). Prevalence of wormian bones in drie adult human skulls: an osteo-morphometric study in Nepal. Jan;94(1):101-109.

Caixia W, Xiaoke H, Yan G, Yinglu J (2015). ZnO Nanoparticles Treatment Induces Apoptosis by increasing Intracellular ROS Levels in LTEP-a-2 Cells BioMed Research International, (9): 432-487,

Chandrasekaran J, Brumin M, Wolf D, Leibman D, Klap C, Pearlsman M (2016). Development of broad virus resistance in non-transgenic cucumber using CRISPR/Cas9 technology.*Mol. Plant Pathol.*17 1140–1153

Chang PK, Ehrlich KC (2010). What does genetic diversity of Aspergillus flavus tell us about *Aspergillus oryzae*? International Journal Food Microbiol 138:189-99.

Ghareib MM, Attia M, Awad N. M, Matter MZ, El-Kahky D (2015). Screening of *Fusarium* spp Resistance to Silver Ions for Ability to Synthesize Silver Nanoparticles from Egyptian Soils. Global Advanced Research Journals 4(9) pp. 366-382.

Happy A, Venkat S, Kumar S, kumar R (2017). A review on green synthesis of zinc oxide nanoparticles –An eco-friendly approach Resource-Efficient Technologies 3: 406–413.

Hinrikson HP, Hurst SF, de Aguirre L, Morrison CJ (2014). Identification of Aspergillus terreus using 18S rRNA gene sequence, Asian Journal of Biochemical and Pharmaceutical Research 4: 2231-2560.

Jeevan R, Cromwell DA, Trivella M (2012). Reoperation Rates after Breast-Conserving Surgery for Breast Cancer among Women in England: Retrospective Study of Hospital Episode Statistics. BMJ, 345, e4505. http://dx.doi.org/10.1136/bmj.e4505

Jesline A, Neetu P, John PM, Narayanan C, Murugan VS (2015). Antimicrobial activity of zinc and titanium dioxide nanoparticles against biofilm-producing methicillin-resistant Staphylococcus aureus Appl Nanosci 5:157–162

Jiang HS, Qiu X N, Li GB, Li W, Yin LY (2014). Silver nanoparticles induced accumulation of reactive oxygen species and alteration of antioxidant systems in the aquatic plant *Spirodela polyrhiza*. Environ Toxicol Chem 33:1398-1405

Kumar HK, Savalgi VP (2017). Microbial Synthesis of Zinc Nanoparticles Using Fungus Isolated from Rhizosphere Soil. *Int. J. Curr. Microbiol. App. Sci.* 6(12): 2359-2364.

Kurtzman CP, Smilley M J, Robnett CJ, Wicklow DT (1986). DNA relatedness among wild and domesticated species in the Aspergillus flavus group. Mycologia 78: 955e9.

Navin N, Krasnitz A, Rodgers L, Cook K, Meth J, Kendall J, Riggs M, Eberling Y, Troge J, Grubor V (2010). Inferring tumor progression from genomic heterogeneity. *Genome Res.* 20, 68–80.

Nei M, Li WH (1979) Mathematical Model for Studying Genetic Variation in Terms of Restriction Endonucleases. Proceedings of the National Academy of Sciences of the United States of America, 76, 5269-5273

Prasanth LA, Nathaniel K, Rémi M (2015). Fast LSTD using stochastic approximation: Finite-time analysis and application to traffic control. In Joint European Conference on Machine Learning and Knowledge Discovery in Databases, pages 66–81. Springer,

Premanathan M, Karthikeyan K, Jeyasubramanian K, Manivannan G (2011). Selective toxicity of ZnO nanoparticles toward Gram-positivebacteria and cancer cells by apoptosis through lipid peroxidation. Nanomedicine: Nanotech. Biol. Med.7: 184–192.

Rajan A, Cherian E, Baskar G (2016). Biosynthesis of zinc oxide nanoparticles using *Aspergillus fumigatus* JCF and its antibacterial activity International Journal of Modern Science and Technology 2: 52-57.

Sammons DW, Adams LD, Nishizawa EE (1981). Ultrasensitive silver-basedcolour staining of polypeptides in polyacrylamide gels. *Electrophoresis*, 2:135-141.

Sangappa M, Vandana SP, Bharath AU, Thiagarajan P (2013). Mycobiosynthesis of novel nontoxic zinc oxide nanoparticles by a new soil fungus *Aspergillus terreus* VIT Journal of Chemical and Pharmaceutical Research, 5(12):1155-1161

Sharmila Bhanu P, Devi Sankar K, Shanthi V, Sujatha K, Subhadra DV (2017). Evaluation of biochemical and immunohistochemical placental antioxidant status in normal and gestational diabetes mellitus mothers International Journal of Anatomy and Research, Vol 5(3.1):4082-89.

Sneath PHA, Sokal RR (1973). Numerical Taxonomy: The Principles and Pratice of Numerical Classification Freeman.(7): 418-573.

Vijayakumar S, Malaikozhundan B, Shanthi S (2018).Control of biofilm-forming clinically important bacteria by green synthesized ZnO nanoparticles and its ecotoxicity on *Ceriodaphnia cornuta*. *Microb Pathogenesis* , 107:88–97.

Williams DB, (1996). Transmission Electron Microscopy. *Material Science, Plenum Press*,4:571-625.

Zhang Y, Yan L, Xu W, Guo X, Cui L, Gao L, Wei Q, Du B (2014). Adsorption of Pb (II) and Hg (II) from aqueous solution using magnetic CoFe2O4 reduced graphene oxide. Journal Mol. Liq. 191:177–182.